

# How Does Pressure Affect Barrier Compression and Isotope Effects in an Enzymatic Hydrogen Tunneling Reaction?\*

Linus O. Johannissen,\* Nigel S. Scrutton, and Michael J. Sutcliffe\*

The shape of the reaction barrier is crucial for enzymatic hydrogen tunneling reactions. Thus, the concept of barrier compression is of fundamental importance. Such compression is believed to arise from “promoting vibrations”—rapid, sub-picosecond donor–acceptor (DA) vibrational modes that transiently compress the reaction barrier, thus enhancing the probability of tunneling and of over-the-barrier transfers and hence the rate of H-transfer.<sup>[1–4]</sup> For reactions that are dominated by H-tunneling, this has experimentally observable impact on the kinetic isotope effect (KIE) and its temperature-dependence,  $\Delta\Delta H^\ddagger$ .<sup>[5,6]</sup> by shortening the tunneling distance, DA compression decreases the KIE, while the temperature-dependence of the vibration gives rise to an elevated  $\Delta\Delta H^\ddagger$ . However, the role of promoting vibrations in H-tunneling reactions is highly contentious.<sup>[2,7–11]</sup> We present a computational study on the effect of pressure on DA compression in an enzymatic H-tunneling reaction, demonstrating that experimental observations are directly coupled to the promoting vibration.

The hydride transfer in the reductive half-reaction of morphinone reductase (MR) has been well characterized, with both experimental and computational studies suggesting that a promoting vibration is required to achieve tunneling.<sup>[12–15,17]</sup> Two recent experimental studies on MR have focused on the effect of mutation<sup>[14]</sup> and hydrostatic pressure<sup>[15]</sup> on the equilibrium donor–acceptor distance (DAD). These revealed a complex, even counter-intuitive, effect on the KIE which can be explained by concomitant changes to the promoting vibration. However, such changes cannot be measured directly. Hay et al.<sup>[15]</sup> observed an increase in primary KIE with pressure, no change in  $\Delta\Delta H^\ddagger$ , and a modest increase in rate constant, and accounted for these effects by invoking an ad-hoc increase in the force constant

for a “soft” (low-frequency) promoting vibration accompanied by a decreased average DAD. The kinetics could thus be modeled using a nonadiabatic, vibronic tunneling formalism,<sup>[16]</sup> but this required a very large decrease in DAD of 0.7 Å from 1 bar to 2 kbar, which is inconsistent with molecular dynamics (MD) simulations.<sup>[17]</sup> A subsequent phenomenological model allowed for a more realistic decrease in DAD of 0.07 Å, although this model overestimates the increase in rate constant by several orders of magnitude.<sup>[18]</sup> Also, the hypothesized increase in force constant with pressure has recently been challenged by Warshel and co-workers.<sup>[19]</sup> Here, we computationally identify the promoting vibration for this H-transfer and analyze how it changes with pressure, and use this information to reproduce the experimentally observed trends in kinetics.

We ran constant-pressure MD simulations of MR with bound coenzyme nicotinamide adenine dinucleotide (NADH) and cofactor flavin mononucleotide (FMN) at 1 bar, 1 kbar, and 2 kbar. The decrease in DAD with increasing pressure is similar to that observed previously (Supporting Information, Figure S1).<sup>[17]</sup> To analyze DA fluctuations at each pressure, spectral densities for DA compression over a 3 ns window were calculated (Figure 1). These

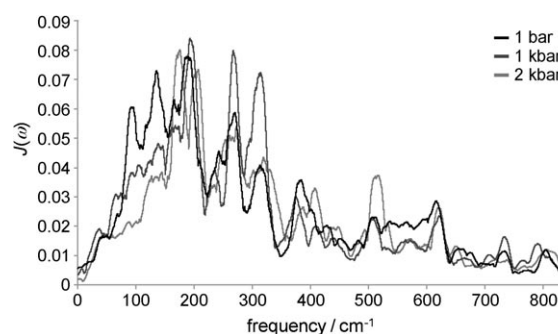


**Figure 1.** Spectral densities for DA compression in MR at 1 bar, 1 kbar, and 2 kbar.

show the magnitude and frequencies of the quasi-harmonic modes that contribute to DA compression (see Supporting Information for details on MD simulations and spectral densities). The magnitude  $J(\omega)$  of the spectral density follows the relationship  $J(\omega) \propto (A\omega)^2$ , where  $\omega$  is the angular frequency and  $A$  the amplitude of the motion—that is, lower-frequency peaks correspond to the largest amplitude motion. At 1 bar, the most significant modes (in terms of magnitude of compression) are therefore those below

[\*] L. O. Johannissen, Prof. M. J. Sutcliffe  
School of Chemical Engineering and Analytical Science  
Manchester Interdisciplinary Biocentre  
131 Princess Street, Manchester M1 7DN (UK)  
Fax: (+44) 161-306-8918  
E-mail: linus.johannissen@manchester.ac.uk  
mike.sutcliffe@manchester.ac.uk

Prof. N. S. Scrutton  
Faculty of Life Sciences  
Manchester Interdisciplinary Biocentre (UK)

[\*\*] This work was supported by the UK Biotechnology and Biological Sciences Research Council (BBSRC). We thank Dr. Sam Hay for useful discussions. N.S.S. is a BBSRC Professorial Fellow and Royal Society Wolfson Merit Award holder.

Supporting information for this article (details of MD simulations, spectral density calculations, and numerical modeling) is available on the WWW under <http://dx.doi.org/10.1002/anie.201006668>.

200 cm<sup>-1</sup>, with the mode at 90 cm<sup>-1</sup> contributing the most to DA compression.

To qualitatively analyze the nature of these low-frequency modes we carried out digital filtering by frequency deconvolution<sup>[20,21]</sup> to remove motions outside the 70–220 cm<sup>-1</sup> range. While the overall (unfiltered) C4 motion does not show a strong correlation to C4–N5 distance (Figure S2), the filtered motion, which represents the majority of compression, is symmetrically coupled to C4–N5 compression (Figure 2B).

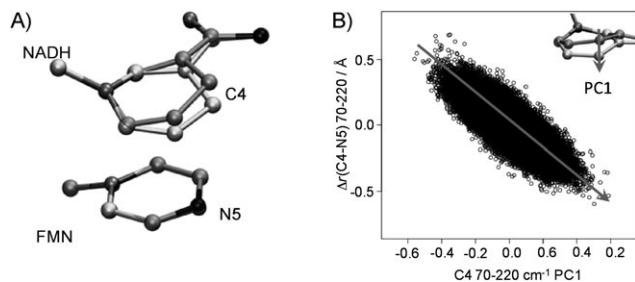


**Figure 2.** Promoting vibration at 1 bar. A) Motion of donor and acceptor groups at 70–220 cm<sup>-1</sup> calculated from average structures at the extremes of this filtered motion. B) Correlation of C4–N5 compression with the first principal component, PC1, of the 70–220 cm<sup>-1</sup> C4 motion ( $R^2 = 0.81$ ); the grey arrows indicate the direction of PC1. A comparison with the unfiltered motion is shown in Figure S2.

Average structures were calculated for the 750 structures (0.5% of the total) at the extremes of this motion (Figure 2B), which revealed that this motion corresponds principally to a bending of the donor nicotinamide ring, with very little motion of the FMN acceptor (Figure 2). This is very similar to a 89 cm<sup>-1</sup> bending mode identified in an MP2 frequency calculation of the nicotinamide, which is the only vibration below 500 cm<sup>-1</sup> with a strong out-of-plane component at C4 (Figure S3). The nature of this motion—a bending of the donor nicotinamide towards the acceptor nitrogen—is similar to a motion previously found to be required for H-transfer.<sup>[13]</sup>

Spectral densities for C4 and N5 motion projected on to the unit vector along the C4–N5 axis reveal that the lowest frequency peaks do indeed correspond mainly to motion of the donor group (Figure 3A and Figure S4). There is an upward shift in frequency for these peaks with increasing pressure (Figure 3B), which causes the decrease in the magnitude of the lowest frequency peaks (at 90 and 140 cm<sup>-1</sup>) in the DA compression spectral density (Figure 1). In other words, this increase in frequency causes the overall degree of compression to decrease with pressure, as illustrated in Figure 4.

While the DA spectral densities show many compressive modes we can define a single promoting vibration as the effective quasi-harmonic mode that describes the overall compression. The frequency for this mode is calculated by mass-weighting the spectral densities according to the relative contribution to the overall compression:

$$\omega_{\text{eff}} = \frac{\int J(\omega) d\omega}{\int J(\omega) / \omega d\omega} \quad (1)$$

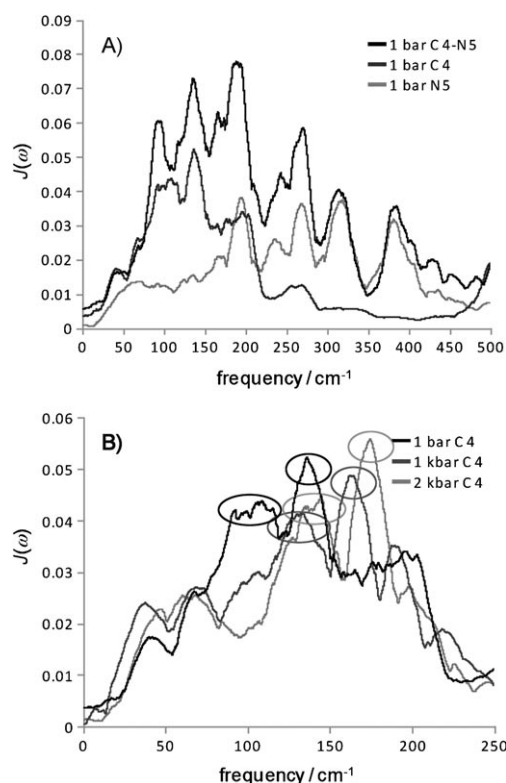


**Figure 3.** A) Comparing the donor–acceptor spectral density (black) to the C4 (dark grey) and N5 (light grey) spectral densities at 1 bar; similar plots for all three pressures are shown in Figure S4. B) C4 spectral densities at 1 bar (black), 1 kbar (dark grey), and 2 kbar (light grey); the ovals highlight the two major peaks at each frequency.

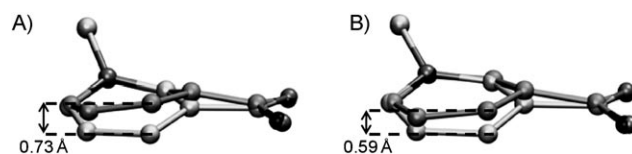


**Figure 4.** Comparing the promoting vibration at A) 1 bar and B) 2 kbar, calculated as per Figure 2A.

This gives effective frequencies ( $f_{\text{eff}} = \omega_{\text{eff}}/2\pi$ ) of 134, 146, and 180 cm<sup>-1</sup> at 1 bar, 1 kbar, and 2 kbar, respectively, which corresponds roughly to the average of the two major low-frequency peaks in the C4 spectral densities (Figure 3B). The 1 bar frequency is lower than the promoting vibrations at 165 cm<sup>-1</sup> in aromatic amine dehydrogenase (AADH),<sup>[21]</sup> 150 cm<sup>-1</sup> in horse liver alcohol dehydrogenase (hLADH), 350–400 cm<sup>-1</sup> in soybean lipoxygenase-1 (SLO-1),<sup>[6,22]</sup> and 160 cm<sup>-1</sup> in human purine nucleoside phosphorylase (hPNP),<sup>[23]</sup> consistent with the soft promoting vibration inferred from experiment.<sup>[15]</sup>

The force constants  $\kappa_{\text{DA}}$  for the promoting vibrations can be calculated from the frequencies and thermal energy (one degree of freedom has an average kinetic energy of  $\frac{1}{2} k_B T$ ):

$$\kappa_{\text{DA}} = k_B T / \langle \Delta r_{\text{DA}} \rangle^2 \quad (2)$$

$$\langle \Delta r_{\text{DA}} \rangle = \langle v_{\text{DA}} \rangle / \omega_{\text{eff}} \quad (3)$$

where  $\Delta r_{\text{DA}}$  is the displacement along DA compression,  $v_{\text{DA}}$  the relative donor–acceptor velocity along the donor–acceptor axis and the angle brackets denote time average. Table 1 summarizes these results, showing that the increase in

**Table 1:** Calculating force constants from MD simulations and spectral densities.

	$f_{\text{eff}}$ [cm <sup>-1</sup> ] <sup>[a]</sup>	$\langle v_{\text{DA}} \rangle$ [m s <sup>-1</sup> ] <sup>[b]</sup>	$\kappa_{\text{DA}}$ [J m <sup>-2</sup> ]
1 bar	134	468	12.0
1 kbar	146	465	14.5
2 kbar	180	452	23.2

[a] From spectral densities [Eq. (1)]. [b] From MD simulations.

$f_{\text{eff}}$  with pressure is accompanied by an increase in  $\kappa_{\text{DA}}$  from 12.0 to 23.2 J m<sup>-2</sup> over the 2 kbar pressure range. The effective reduced masses  $m_{\text{eff}}$  for these modes are 11.3, 11.4, and 12.1 amu ( $\kappa_{\text{DA}} = m_{\text{eff}} \omega_{\text{eff}}^2$ ). This relatively low mass, similar to the 14 amu obtained by Hammes-Schiffer and co-workers for SLO-1,<sup>[6]</sup> suggests that this is a localized vibration. However, it also suggests that the promoting vibration involves more than just a bending of the nicotinamide group shown in Figure 2 (the MP2 frequency calculation of the nicotinamide analogue shows a reduced mass of 2.6 amu for the 89 cm<sup>-1</sup> bending mode).

The calculated  $\kappa_{\text{DA}}$  values are similar to those estimated by Hay et al. from experiment (5 J m<sup>-2</sup> at 1 bar and 14 J m<sup>-2</sup> at 2 kbar).<sup>[15]</sup> However, Hay et al. used a harmonic approximation for the H wavefunctions in their vibronic tunneling model, which required a very large decrease in  $r_0$ —the equilibrium reactant–product well separation at a configuration compatible with tunneling. Here, we instead employed a vibronic formalism with more accurate Morse potentials; the modeling is described in detail in Refs. [5,25] and in the Supporting Information. In short, the rate depends on the H nuclear wavefunction overlap between the reactant and product states, which is in turn governed by  $\kappa_{\text{DA}}$  and  $r_0$ .<sup>[16,24,25]</sup> The results are summarized in Figure 5 and Table 2.

The modeling was performed by modifying  $r_0$  until the best fit to  $\Delta\Delta H^\ddagger$  and KIE from Hay et al.<sup>[15]</sup> and  $\kappa_{\text{DA}}$  from Equations (2) and (3) could be obtained. The resulting decrease in  $r_0$  values is similar to the decrease in DAD from the MD simulations (0.22 Å cf. 0.1 Å; Figure S1). Crucially, the increasing KIEs were reproduced with  $\kappa_{\text{DA}}$  values very similar to those calculated and (nearly) constant  $\Delta\Delta H^\ddagger$ . Additionally, Hay et al. measured a factor of 3.2 increase in rate constant  $k_{\text{H}}$  from 1 bar to 2 kbar.<sup>[15]</sup> This increase in  $k_{\text{H}}$  is unlikely to be caused by an increase in driving force or a

**Table 2:** Parameters ( $\kappa_{\text{DA}}$  and  $r_0$ ) used for modeling the KIE,  $\Delta\Delta H^\ddagger$ , and relative rate constants for H-transfer,  $k_{\text{H,rel}}$  at 1 bar, 1 kbar, and 2 kbar.

	$r_0$ [Å]	$\kappa_{\text{DA}}$ [J m <sup>-2</sup> ]	KIE	$\Delta\Delta H^\ddagger$ [kJ mol <sup>-1</sup> ]	$k_{\text{H,rel}}$
1 bar	1.07	13.3	4.04	5.03	1.00
1 kbar	0.98	16.8	4.84	5.44	1.45
2 kbar	0.85	22.5	5.38	5.34	5.93

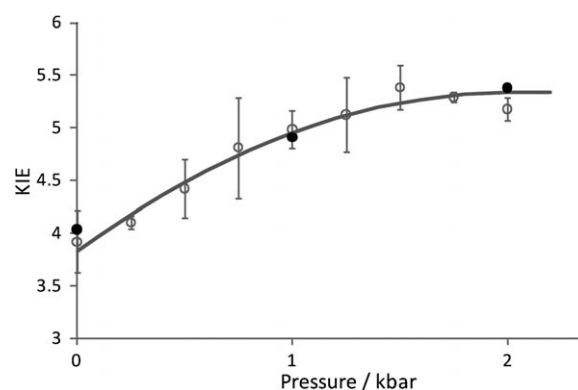


**Figure 5.** Experimental KIEs from Hay et al.<sup>[15]</sup> (open circles) with standard error, fits to a phenomenological vibronic model that incorporates a pressure-dependent force constant<sup>[18]</sup> (solid line), and modeled KIEs (filled circles) versus pressure.

decrease in reorganization energy: an increase in pressure is unlikely to facilitate reorganizational fluctuations,<sup>[26]</sup> and it has previously been shown that this H-transfer is not affected by solvent effects (changes in pH, dielectric constant, or viscosity).<sup>[27,28]</sup> Therefore this increase in  $k_{\text{H}}$  is most likely due to changes in DAD and  $\kappa_{\text{DA}}$ , and is reproduced very closely here (note that only the relative rates are shown since the absolute rates depend on unknown parameters—electronic coupling, driving force, and reorganization energy). These results highlight the complex relationship between donor–acceptor compression and KIEs. In the absence of a promoting vibration (i.e. a “static” tunneling distance), the KIE decreases exponentially with decreasing tunneling distance—here, because the decrease in  $r_0$  is offset by an increase in  $\kappa_{\text{DA}}$ , the increase in rate (and therefore decrease in the average tunneling distance) is instead accompanied by an increase in the KIE.

In conclusion, the promoting vibration for the H-transfer between NADH and FMN in MR has been characterized as an out-of-plane bending of the nicotinamide, and the effect of pressure on this compressive motion has been quantitatively assessed. The decrease in DAD with pressure is accompanied by an increase in force constant  $\kappa_{\text{DA}}$ , and therefore an increase in the free energy, for this compression. The decrease in magnitude of DA compression is accompanied by a significant increase in frequency. The change in DAD and  $\kappa_{\text{DA}}$  is consistent with the experimentally observed increase in KIE, constant  $\Delta\Delta H^\ddagger$  and increase in rate. These results show a strong qualitative agreement with previous phenomenological pressure dependency studies on MR,<sup>[15,18]</sup> demonstrating the value of KIE and  $\Delta\Delta H^\ddagger$  and their pressure dependencies as probes for promoting vibrations and barrier compression, and our results highlight the complex relationship between DA compression and KIEs.

Received: October 23, 2010

Published online: January 25, 2011

**Keywords:** compressive modes · enzyme catalysis · H-tunneling · kinetic isotope effect · promoting vibrations

- [1] D. Antoniou, S. D. Schwartz, *J. Chem. Phys.* **1998**, *108*, 3620.
- [2] J. E. Basner, S. D. Schwartz, *J. Am. Chem. Soc.* **2005**, *127*, 13822.
- [3] J. H. Skone, A. V. Soudackov, S. Hammes-Schiffer, *J. Am. Chem. Soc.* **2006**, *128*, 16655.
- [4] S. Hay, L. O. Johannissen, M. J. Sutcliffe, N. S. Scrutton, *Biophys. J.* **2010**, *98*, 121.
- [5] M. J. Knapp, J. P. Klinman, *Eur. J. Biochem.* **2002**, *269*, 3113.
- [6] E. Hatcher, A. V. Soudackov, S. Hammes-Schiffer, *J. Am. Chem. Soc.* **2007**, *129*, 187.
- [7] S. Hammes-Schiffer, S. J. Benkovic, *Annu. Rev. Biochem.* **2006**, *75*, 519.
- [8] M. H. Olsson, W. W. Parson, A. Warshel, *Chem. Rev.* **2006**, *106*, 1737.
- [9] Z. D. Nagel, J. P. Klinman, *Chem. Rev.* **2006**, *106*, 3095.
- [10] A. Warshel, P. K. Sharma, M. Kato, Y. Xiang, H. Liu, M. H. Olsson, *Chem. Rev.* **2006**, *106*, 3210.
- [11] S. D. Schwartz, V. L. Schramm, *Nat. Chem. Biol.* **2009**, *5*, 551.
- [12] J. Basran, R. J. Harris, M. J. Sutcliffe, N. S. Scrutton, *J. Biol. Chem.* **2003**, *278*, 43973.
- [13] J. Pang, S. Hay, N. S. Scrutton, M. J. Sutcliffe, *J. Am. Chem. Soc.* **2008**, *130*, 7092.
- [14] C. R. Pudney, L. O. Johannissen, M. J. Sutcliffe, S. Hay, N. S. Scrutton, *J. Am. Chem. Soc.* **2010**, *132*, 11329.
- [15] S. Hay, M. J. Sutcliffe, N. S. Scrutton, *Proc. Natl. Acad. Sci. USA* **2007**, *104*, 507.
- [16] A. M. Kuznetsov, J. Ulstrup, *Can. J. Chem.* **1999**, *77*, 1085.
- [17] S. Hay, C. R. Pudney, T. A. McGrory, J. Pang, M. J. Sutcliffe, N. S. Scrutton, *Angew. Chem.* **2009**, *121*, 1480; *Angew. Chem. Int. Ed.* **2009**, *48*, 1452.
- [18] S. Hay, N. S. Scrutton, *Biochemistry* **2008**, *47*, 9880.
- [19] S. C. L. Kamerlin, J. Mavri, A. Warshel, *FEBS Lett.* **2010**, *584*, 2759.
- [20] R. B. Sessions, P. Dauber-Osguthorpe, D. J. Osguthorpe, *J. Mol. Biol.* **1989**, *210*, 617.
- [21] L. O. Johannissen, S. Hay, N. S. Scrutton, M. J. Sutcliffe, *J. Phys. Chem. B* **2007**, *111*, 2631.
- [22] S. Caratzoulas, J. S. Mincer, S. D. Schwartz, *J. Am. Chem. Soc.* **2002**, *124*, 3270.
- [23] S. Núñez, D. Antoniou, V. L. Schramm, S. D. Schwartz, *J. Am. Chem. Soc.* **2004**, *126*, 15720.
- [24] M. P. Meyer, J. P. Klinman, *Chem. Phys.* **2005**, *319*, 283.
- [25] L. O. Johannissen, T. Irebo, M. Sjöin, O. Johansson, L. Hammarström, *J. Phys. Chem. B* **2009**, *113*, 16214.
- [26] L. Meinhold, J. C. Smith, A. Kitao, A. H. Zewail, *Proc. Natl. Acad. Sci. USA* **2007**, *104*, 17261.
- [27] S. Hay, C. R. Pudney, M. J. Sutcliffe, N. S. Scrutton, *ChemPhys-Chem* **2008**, *9*, 1875.
- [28] S. Hay, C. R. Pudney, M. J. Sutcliffe, N. S. Scrutton, *Angew. Chem.* **2008**, *120*, 547; *Angew. Chem. Int. Ed.* **2008**, *47*, 537.